Allogeneic Treg-derived artificial vesicles: A promising therapeutic modality for multiple sclerosis

Irina Alekseevna Ganeeva[1], Elvina Maratovna Gilyazova[1], Arthur Ajdarovich Khannanov[2], Mariia Eugenievna Nektorova[1], Alexey Michailovich Rogov[1], Timur Ildarovich Khaibullin[3], Ekaterina Anatolievna Zmievskaya[1*], Emil Rafaelevich Bulatov[1,4]

[1]Institute of Fundamental Medicine and Biology, Kazan Federal University, Kazan 420008, Russia
[2]A.M. Butlerov Institute of Chemistry, Kazan Federal University, Kazan 420008, Russia
[3]Kazan State Medical Academy, Neurology Department, Kazan 420012, Russia
[4]Shemyakin-Ovchinnikov Institute of Bioorganic Chemistry, Russian Academy of Sciences, Moscow 117997, Russia

Article Info

Abstract

Introduction: Multiple sclerosis (MS) is a chronic autoimmune disease of the central nervous system (CNS). $CD4^+CD25^{+hi}$ Tregs, which normally suppress immune responses, exhibit impaired function in MS. Treg-derived extracellular vesicles (EVs) carry immunoregulatory proteins and miRNAs that modulate T-cell activity. However, EVs from MS patients show reduced suppressive capacity, suggesting their dysfunction contributes to MS pathogenesis. This highlights EVs' potential role in MS development and therapy.

Methods: Tregs were differentiated from naïve T cells isolated from peripheral blood mononuclear cells (PBMCs) of healthy donor, then transduced with B2M-shRNA lentivirus to generate HLA class I-knockdown Tregs. Extracellular vesicles—including natural vesicles, cytochalasin B-induced artificial vesicles, and ultrasound-induced artificial vesicles—were isolated from Tregs and characterized by scanning electron microscopy (SEM), nanoparticle tracking analysis (NTA), flow cytometry, and Western blot. Their effects on healthy donor and MS patient PBMCs were evaluated via flow cytometry and ELISA (IL-6, IL-10, IFN-γ).

Results: Ultrasonication yielded a higher number of vesicles enriched with key immunosuppressive proteins, including PD-1 and Tim-3, compared to cytochalasin B. Functional assays demonstrated the ability of ultrasonication-induced AVs to suppress inflammatory markers, such as IFNγ, and modulate the cytokine profile in both healthy and MS-derived PBMCs.

Conclusion: Developing effective MS therapies remains challenging. While cellular therapies face limitations like Treg dysfunction and CNS delivery issues, allogeneic EVs offer a promising alternative due to their scalability, low immunogenicity, and blood-brain barrier penetration. We developed Treg-derived artificial vesicles (TrAVs) that maintain immunosuppressive properties and modulate PBMC responses, suggesting therapeutic potential for MS. Further research is needed to optimize production and validate efficacy in disease models.
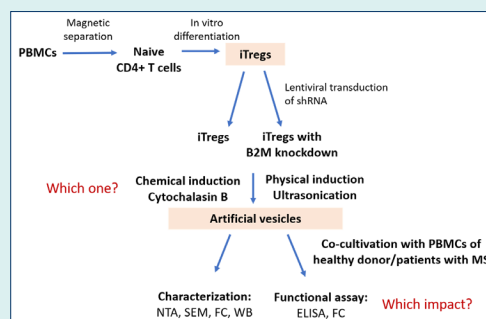
Introduction

Multiple sclerosis (MS) is a progressive neurological disease, affecting 2.8 million people worldwide in 2020. This number has increased by 20% compared to 2013 data provided by the Multiple Sclerosis International Federation.[1]

MS is a cell-mediated autoimmune disease directed against myelin antigens of the central nervous system (CNS),[2] involving different types of immune cells in the pathogenesis. Despite many studies and the autoimmune nature of the disease, the initiating autoantigen in MS is unknown. This is explained by the fact that in diagnosed multiple sclerosis there is no single autoantigen that could be targeted, since reactivity spreads to other organ-

*Corresponding author: Ekaterina Anatolievna Zmievskaya, Email: ekazmievskaya@gmail.com

specific antigens as inflammation progresses.[3]

In MS, circulating regulatory CD4+Foxp3+Tregs exhibit abnormally reduced immunoregulatory capacity. One possible mechanism for the functional deficiency of Tregs associated with MS is their excessive propensity to acquire a Th1 phenotype (Th1-Treg); this phenotype is less regulatory than standard Tregs. In addition, IL-6 secreted by proinflammatory cells leads to a decrease in their regulatory function.[4]

Thus, the role of CD4+CD25hi Tregs in the pathogenesis of MS, expressed in the partial loss of their normal immunosuppressive function, is generally recognized.[5]

Chwojnicki et al clinically demonstrated the promise of using ex vivo expanded autologous Tregs, while emphasizing the importance of ensuring their entry into the central nervous system to provide a therapeutic effect.[6] One approach in this regard may be the use of vesicles obtained from Tregs. EVs are actively studied as cell-free biosimilars and drug delivery vehicles. In parallel with this, many methods of inducing EVs formation are being studied - both natural (passive secretion, cell activation) and stress (hunger, hypoxia, mechanical action, chemical agents etc.) to increase the efficiency of their release from precursor cells.[7,8] Moreover, the ability of EVs to penetrate the blood-brain barrier is actively studied by many scientists in various areas.[9-11]

Tregs play a crucial role in MS pathogenesis. These cells produce EVs enriched with proteins and RNA molecules capable of modulating T-cell proliferation and survival. Importantly, research has shown that the immunosuppressive capacity of Treg-derived EVs is significantly diminished in MS patients, suggesting their involvement in disease mechanisms.[12] While the exact nature of this EV dysfunction remains unknown, therapeutic administration of healthy donor-derived allogeneic Treg EVs could potentially compensate for this regulatory deficiency in MS patients.

The main physical methods for inducing vesicle formation include mechanical action (vibrational stress), high-frequency ultrasound, and radiation.[13] Among these methods, ultrasound treatment is of particular interest, as it is a widely used tool for producing microvesicles (MV)[14]. Numerous studies have demonstrated that ultrasound exposure of cell cultures leads to a significant increase in microvesicle secretion.[15,16] This effect is explained by the ability of ultrasound waves to cause temporary destabilization of the cell membrane, which stimulates the vesicle budding process. In addition, this method allows for the production of vesicles with specified characteristics, which is especially important for their subsequent therapeutic use. However, further research is required to optimize ultrasonic processing protocols and standardize the resulting products.

Thus, the development and study of a vesicular drug based on Treg for the treatment of multiple sclerosis is a relevant area in cell therapy of autoimmune diseases. However, the cornerstone of the use of such therapy is its quantity, which can be overcome by using various methods of chemical or physical induction of the release of extracellular vesicles, which is also envisaged within the framework of this work.

In this study, we present a novel strategy for developing artificial vesicles (AVs) derived from in vitro differentiated Tregs. The approach integrates three key components: (1) differentiation of naive CD4+T cells from healthy donors into functional iTregs, (2) knockdown of β2-microglobulin (B2M) to reduce immunogenicity and improve allogeneic compatibility, and (3) induction of AVs using chemical and physical methods. The generated AVs were thoroughly characterized for their structural, molecular, and functional properties and assessed for their potential to modulate immune responses in vitro using peripheral blood mononuclear cells (PBMCs) from both healthy donors and MS patients. Important criteria for evaluating such AVs are parameters such as the efficiency of B2M knockdown, which is important for reducing immunogenicity. Also important is the transfer of key suppressor molecules by these vesicles, such as LAG-3, Tim-3, CTLA-4, and PD-1, since these are the main molecules through which Tregs exert a suppressor effect on other immune cells. In addition, it is necessary to confirm the non-apoptotic nature of the vesicles, since apoptotic bodies have a size similar to some vesicle fractions and can be immunogenic.

This work highlights the potential of Treg-derived AVs as a scalable, biosafe, and effective therapeutic modality for autoimmune diseases, addressing critical barriers associated with cell-based therapies.

Materials and Methods
Naive T cells separation and iTregs differentiation
PBMCs were obtained from whole blood of healthy donors by centrifugation on Ficoll gradient with a density of 1.077 g/mL (Paneco, Russia) at 800 g for 30 minutes. The buffy coat was collected and washed twice with Dulbecco's phosphate-buffered saline (DPBS). Then the cells were counted in a Neubauer chamber with trypan blue staining (Thermo Fisher, USA). MojoSort™ Human CD4 Naïve T Cell Isolation Kit (Biolegend, USA) was used for naive CD4+T cells negative magnetic separation. Then cells were seeded in RPMI-1640 nutrient medium with L-glutamine, penicillin-streptomycin (Paneco, Russia) and the addition of 10% fetal bovine serum (FBS) (Biosera, France), IL-2 at 300 IU /mL (Prospec, Israel) and 10 ng /mL TGF-b (BioLegend, USA). To activate naive T cells, they were seeded at a concentration of 2×10^6 cells/mL and T-cell TransAct (Miltenyi, USA) according to the manufacturer's protocol was added for 48 hours. For iTreg differentiation TGFβ at concentration 10 ug /mL was used during the whole cultivation period. T cells were

then counted every two days and fresh medium with IL-2 and TGFβ was added to maintain a cell density of about 1×10^6 cells /mL.

Generation of allogeneic iTregs with B2M knockdown

Knockdown was carried out using shRNA to B2M delivered by lentiviral transduction. Lentivirus of 2nd generation was obtained in HEK293T culture using PEI MAX transfection and concentrated using Amicon 15-Ultra 100kDA (Merck, USA). Then lentivirus was used for iTreg transduction at MOI 10 with addition of protamine sulfate at 25 µg /mL and spinoculation at 1500 g, 32 °C, 2 h. After 16 h transduction media was replaced.

Artificial vesicles induction and separation

To obtain naturally secreted EVs as a control, iTreg cells were harvested on day 8 of expansion, washed twice with DPBS, and plated in serum-free AIM-V medium (Thermo Fisher, USA) containing 300 IU /mL IL-2 at a density of 1×10^6 cells /mL. After 48 h of incubation, the conditioned media were collected by centrifugation for subsequent separation of EVs.

To obtain artificial vesicles (AVs), cells were washed twice with DPBS and resuspended in serum-free medium. Then, AVs were induced using either cytochalasin B or ultrasound. For induction with cytochalasin B (Sigma-Aldrich, USA), it was added at a concentration of 10 µg /mL and the cells were incubated in a CO_2 incubator for 30 minutes. The cells were then thoroughly vortexed for 30 seconds. For ultrasound induction, the cells were sonicated using a Qsonica Q125 homogenizer (Qsonica, USA) at 30% power, 1 sec action, 1 sec pause, 1 minute on ice. After induction both AVs groups were purified by the sequential centrifugation: 300 g 10 min, 2000 g 10 min, 20 000 g 20 min. Methodology was optimized in previous work.[17]

Flow cytometry

For flow cytometry, 3×10^5 cells or an aliquot of vesicles were collected and washed twice with DPBS. The cells were stained with antibodies for 20 min and washed twice with DPBS. Vesicle samples were dissolved in DPBS, stained with the lipophilic dye DiD for 15 min, centrifuged to replace the buffer, and stained with the antibodies in the same manner as described for cells. Flow cytometry was performed on a BD FACS Aria III instrument (BD Biosciences, USA).

List of antibodies:

1. Mix: anti-CD3(PerCP-Cy5.5), anti-CD4(FITC), anti-CD25(PE) (Cat# 648956, BD Biosciences)
2. anti-Lag3(PE) (Cat# 565616, BD OptiBuild)
3. anti-Tim-3(BV421) (Cat# 565563, BD Horizon)
4. anti-CTLA-4(PE) (Cat# 555853, BD Biosciences)
5. anti-PD-1(BV510) (Cat# 563076, BD Horizon)
6. anti-HLA-ABC(FITC) (Cat# 555552, BD Pharmingen).

Western blotting

For immunoblotting, samples were subjected to SDS-PAGE electrophoresis in 12% TGX FastCast gel (Bio-Rad, USA) at 70 V and 180 V. 0,8 µg of total protein per well was loaded. A Western C ruler (Bio-Rad, USA) was used for size estimation. Proteins were transferred from the gels to 0.45 µm PVDF membranes (Bio-Rad, USA) using a Mini Trans-Blot Cell (Bio-Rad, USA) at a constant voltage of 17V for 30 min using Turbo Transfer Buffer (Bio-Rad, USA). Free reactive sites were blocked with 5% nonfat dry milk in PBS-Tween solution for 1.5 h at room temperature. The membranes were then washed with PBS-Tween for 4×15 min. The primary antibody to the protein of interest was used overnight at 4 °C at the recommended dilution with slow agitation. The next day, the membranes were washed with PBS-Tween for 4×15 min. HRP-conjugated secondary antibodies were then added at the recommended dilution in 5% milk-PBS-Tween and incubated for 1 hour at room temperature, followed by washing with PBS-Tween for 4×15 min. 1200 mL of Pierce ECL Western Blotting Substrate (Bio-Rad) were then added and the membranes were incubated for 2–5 min. Membrane images were acquired using the ChemiDoc XRS + System (Bio-Rad, USA). Images were processed densitometrically in Image J software to estimate the relative amount of protein content.

List of used antibodies: β-actin (A00730, Genscript, USA), CD3 (ab699, Abcam, USA), Calnexin (MAA280Hu22, Cloud clone, China), HSP70 (AF5466, Affinity, China), Caspase 3 (14220S, Cell Signaling Technology, USA).

Scanning electron microscopy

For SEM, vesicle samples were washed twice and resuspended in 0.1 M sodium phosphate buffer (pH 7.4). They were then deposited on defatted glass slides by centrifugation in a 6-well plate at 700 g for 1 h. Then, the samples were fixed with 10% glutaraldehyde, washed with MQ water and dehydrated according to the following scheme: ethyl alcohol 30%-50%-70%-80%-96% twice for 15 min each. Finally, the slides were dried in the open air. The samples fixed on the holder were placed in the chamber of a Q 150T ES vacuum installation (Quorum Technologies, UK). The conductive layer was applied by cathodic sputtering with an Au/Pd alloy in a ratio of 80/20. The thickness of the applied layer was 15 nm. The measurements were performed on a Merlin high-resolution field emission scanning electron microscope (Carl Zeiss, Germany). The surface morphology was recorded at a primary electron accelerating voltage of 5 kV and a probe current of 300 pA for minimal impact on the object of study.

Nanoparticle tracking analysis

NTA was performed using a NanoSight LM10 nanoparticle

size and content analyzer (Malvern Instruments, UK). The detector was a C11440-50B CMOS camera with an FL-280 image capture sensor (Hamamatsu Photonics, Japan). The measurement method was selected in a pre-cuvette for aqueous solutions equipped with a 405 nm laser (CD version, serial number 2990491) and a Kalrez sealing ring. Temperature was recorded for all measurements using an OMEGA HH804 contact thermometer (Omega Engineering, Taiwan). Samples for analysis were collected and introduced into the measurement cell using a 1 mL two-piece glass syringe through a luer adapter (Hamilton Company, USA). To increase the statistical dose, the sample was pumped through the measurement chamber using a piezoelectric dispenser. Each sample was imaged sequentially six times; the data acquisition time was sequential and continuous for 60 s. The NanoSight LM10 analyzer images were processed using NTA 2.3 software (build 0033). The hydrodynamic diameter was calculated using the two-dimensional Einstein-Stokes equation.

Enzyme-linked immunosorbent assay
ELISA of collected supernatants was performed according to the manufacturer's instructions using the following kits: IL-6 ELISA kit (VectorBEST, Russia), IL-10 ELISA kit (VectorBEST, Russia), IFNγ ELISA kit (VectorBEST, Russia).

Co-cultivation of mononuclear cells with induced T-regulatory cells
For co-cultivation peripheral blood mononuclear cells were collected from one healthy donor and 3 multiple sclerosis patients' blood. Obtained cells were labelled by DiO vybrant dye for further co-cultivation with induced T regulatory cells (iTregs) or iTregs-induced artificial vesicles (TrAVs). For co-cultivation with PBMC all type of cells (PBMCs from healthy donor, PBMCs from MS

patient, iTregs, allo-iTregs) was seeded in the amount of 1×10^6 cells per well, TrAVs were added in amounts of 10 µg /mL and 5 ug /mL phytohemagglutinin (PHA) for cell activation.

Statistical analysis
One-way non parametric ANOVA with Tukey test was used for ELISA with healthy donor and with MS patients. Data analysis was performed using GraphPad Prism 5. In the graphs, P value < 0.05 is marked *, $P < 0.01$ is marked **, and $P < 0.001$ is marked ***.

Results
Characterization of iTregs
On the 10th day after isolation of naive CD4 + T cells from the peripheral blood of a healthy donor, obtained iTreg cells were analysed by flow cytometry to confirm cell differentiation. Tregs CD3$^+$CD4$^+$CD25$^+$phenotype was shown in 86% of the cells of the population, and a high percentage of cells in the population carrying suppressor molecules CTLA-4 (88%) and PD-1 (44%) was also shown (Fig. 1).

Further differentiated iTreg cells were used to obtain EVs and AVs induced by cytochalasin B (ChB TrAVs) or ultrasonication (US TrAVs).

Morphological characterization of TrAVs obtained by cytochalasin B or ultrasonication induction methods
Scanning electron microscopy was performed for three types of samples: extracellular naturally secreted vesicles as comparison control (Fig. 2C), ChB TrAVs (Fig. 2A) and US TrAVs (Fig. 2B). Vesicles obtained by three induction methods are visualised on SEM as spherical structures of various sizes from 10 nm to 500 nm.

According to NTA, the average particle size was found to have close meanings for all samples: EVs have 205 ± 3.1
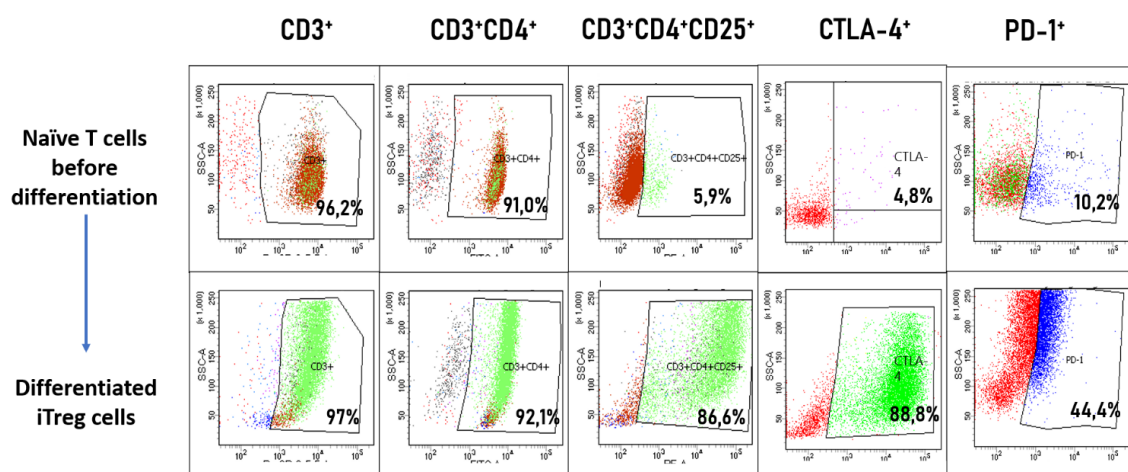

Fig. 1. Phenotypic analysis iTregs by flow cytometry. Naive CD4$^+$T cells were isolated from PBMCs and assessed before (top row) and after 10 days of in vitro differentiation (bottom row). The progression of differentiation was evaluated using the CD3$^+$CD4$^+$CD25$^+$staining panel, indicative of Treg phenotype. Additional markers of immunosuppressive activity, CTLA-4 and PD-1, were analyzed to confirm the acquisition of functional Treg characteristics. The percentage of cells expressing each marker is indicated in the respective gates.
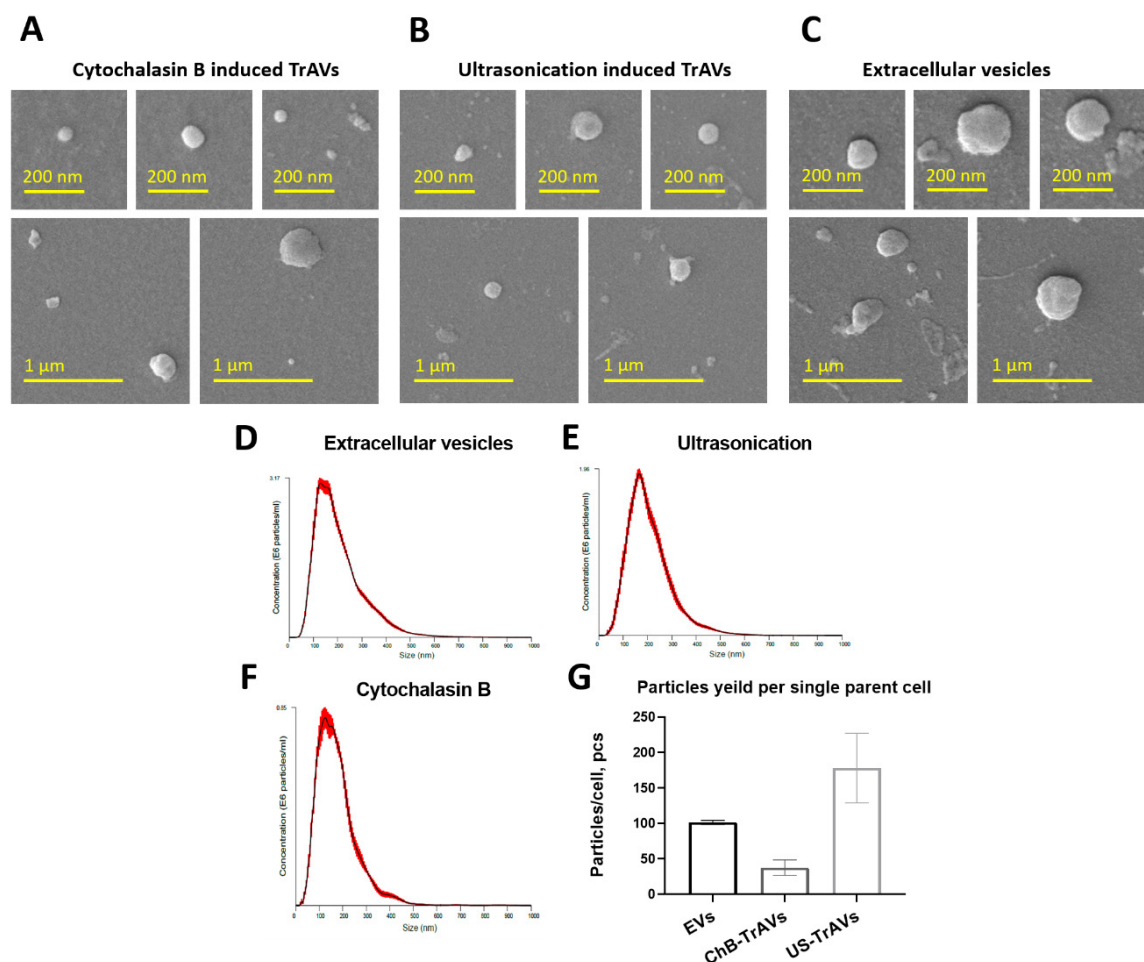
Fig. 2. SEM images, NTA and particle yield comparison of vesicles derived from iTregs. A-C Representative SEM images show three types of vesicles: (A) ChB TrAVs, (B) US TrAVs, and (C) EVs. Vesicles exhibit a spherical morphology with a size range of 10–500 nm, with scale bars indicating either 200 nm or 1 μm, as specified. D-E The images demonstrate differences in vesicle size and uniformity between induction methods and natural secretion. Size distribution profiles of vesicles obtained by different methods: (D) - EVs, (E) - US TrAVs, and (F) - ChB TrAVs. Vesicle size was measured in nanometers, and particle concentration is presented as particles/mL (×10⁶). G - Quantitative comparison of particle yield per parent cell across the three methods. Ultrasonication produced the highest yield of vesicles (178 particles/cell), followed by EVs (101 particles/cell), while cytochalasin B yielded the fewest vesicles (38 particles/cell). Error bars represent standard deviations.

nm mean size, ChB TrAVs - 175 ± 3.9 nm and US TrAVs - 207 ± 5.6 nm. Also, the yield of vesicles per parent cell was calculated for each sample based on source cell number and sample volume (Fig. 2G). The quantitative yield of vesicles (pcs./cell) was: for EVs - 101.45 ± 2.9, for vesicles obtained by cytochalasin B - 37.6 ± 10.9, for vesicles obtained by ultrasonication - 178.14 ± 49.1. Regarding particles polydispersity (Fig. 2D, 2E, 2F), EVs and US TrAVs demonstrate quite similar size distribution while cytochalasin B allows to obtain more uniform vesicles.

Characterization of protein composition of TrAVs obtained by cytochalasin B or ultrasonication induction methods

At the next step Western blot analysis was used for vesicular protein composition characterisation according to MISEV 2023 recommendations.

Western blot analysis showed the absence of caspase-3 in all three vesicle samples, which refutes the apoptotic nature of the vesicles (Fig. 3D). In addition, the sample obtained by ultrasound induction showed a significantly higher content of calnexin (Fig. 3B), a marker of the endoplasmic reticulum, while ChB TrAVs contained only trace amounts of this protein. The content of the cytoplasmic component marker HSP70 in all three samples was quite low (Fig. 3C). At the same time, the presence of the membrane functionally important protein CD3 was observed in all three samples (Fig. 3A), but for artificial vesicles, especially cytochalasin B-induced, at a significantly lower level.

Assessment of functionally important immunosuppressive proteins on the vesicles surface was performed with flow cytometry.

For vesicle detection and gate setting, due to their small size, vesicles stained with the membrane vibrant dye DiD were used as a negative control. In addition, staining with antibodies to LAG3, Tim-3, CTLA-4 and PD-1 was performed in each group (Fig. 4). In addition, a
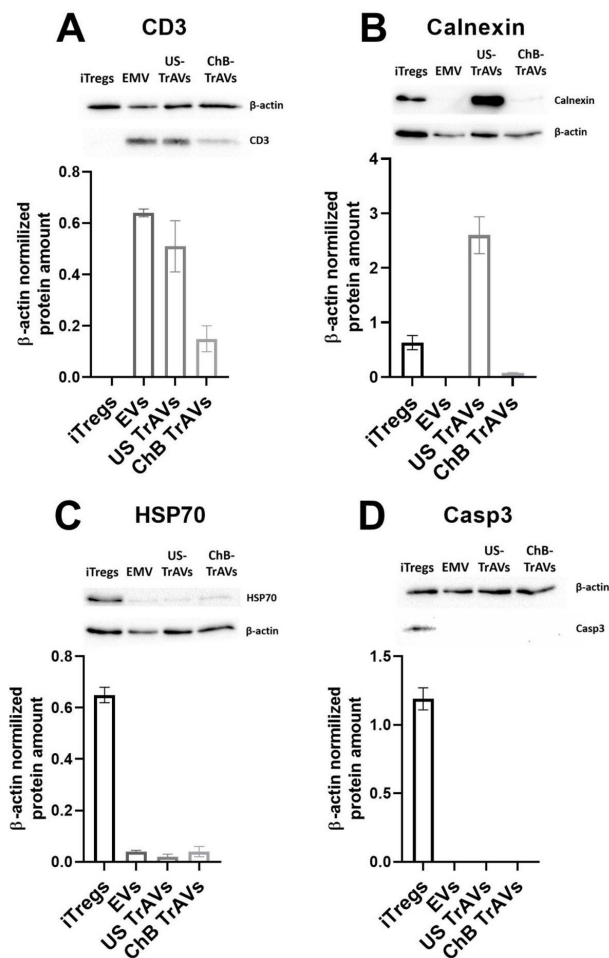
Fig. 3. Western blot analysis of protein markers in vesicles derived from iTreg cells. Protein expression levels were evaluated in EVs, US TrAVs, and ChB TrAVs. Expression levels were normalized to β-actin. (A) CD3: A T cell marker present in all vesicle types but significantly lower in ChB TrAVs. (B) Calnexin: An endoplasmic reticulum marker observed predominantly in US TrAVs, with minimal detection in other vesicle types. (C) HSP70: A cytosolic protein detected at low levels in all vesicle types. (D) Caspase 3: An apoptotic marker absent in all vesicle types, confirming non-apoptotic origin. Error bars represent standard deviations, and bands correspond to representative blots.

cellular control of parent iTreg cells was used. In induced T-regulatory cells, the following cells were positively stained: LAG3 – 9.9%, Tim-3 – 85.6%, CTLA-4 – 88.8%, PD-1 – 24%. In EVs, the following vesicles were positively stained: LAG3 – 0.3%, Tim-3 – 12.4%, CTLA-4 – 0.3%, PD-1 – 4.5%. In the vesicles obtained by ultrasonication, the positively stained vesicles amount was quite similar: LAG3 – 0.2%, Tim-3 – 11.2%, CTLA-4 – 0.4%, PD-1 – 7.1%. In the vesicles obtained by cytochalasin B, the positively stained vesicles were found at lower levels: LAG3 – 0.1%, Tim-3 – 2.6%, CTLA-4 – 0.1%, PD-1 – 3.0%. It was shown that the transfer of functionally important molecules from the surface of induced T-regulatory cells occurs in all three stimulation methods, but cytochalasin B induction is associated with lower efficiency of the transfer of essential suppressor molecules.

For further experiments to evaluate the effect of iTreg vesicles on cells from MS patients, the ultrasound induction mechanism was chosen due to its higher yield and functional correspondence in the presence of suppressor receptors.

Obtaining of allo-iTreg with B2M shRNA knockdown

Knockdown of B2M was preceded with lentiviral transduction of shRNA and confirmed by flow cytometry 48hrs after transduction (Fig. 5). For modified iTregs (allo iTregs) efficacy of knockdown was determined by a decrease in the signal of HLA I positive cells and was 81,7% in allo iTregs (decrease from 96% in non-modified iTregs control to 14%).

Obtained allo iTregs were used for induction of artificial vesicles by ultrasonication for its further functional testing.

Effect of artificial iTreg vesicles on activation of healthy donor's PBMCs

To estimate impact of US TrAVs on PHA-induced activation of autologous healthy donor's PBMCs it was *in vitro* co-cultured with further flow cytometry to assess changes in activation marker CD69 expression on cell surface; ELISA of supernatants was proceeded to assess changes in cytokines secretion (Fig. 6). The same design was implemented to estimate impact of non-modified iTregs and allo iTregs as well as obtained from its ultrasound-induced artificial vesicles (TrAVs and allo TrAVs, respectively) on PHA-induced activation of allogeneic healthy donor's PBMCs (Fig. 7).

Co-cultivation with autologous healthy donor cells showed a slight decrease in the amount of activated CD69 + PBMCs under the influence of autologous Tregs, but more significant for cells co-cultured with US TrAVs (Fig. 6A). Similarly, co-cultivation with non-autologous healthy donor PBMCs showed a decrease in activation with the addition of US TrAVs and allo TrAVs but not its parent cells (Fig. 7A).

The IL-6 concentration in the medium after 24 hours of co-cultivation did not change upon interaction of autologous PBMCs with iTregs and with TrAVs (Fig. 6C). At the same time, when allogeneic PBMCs were used (Fig. 7C), concentration decreased twofold upon co-cultivation with allo iTregs, but not with nonmodified iTregs, and by 25% upon co-cultivation with TrAVs.

IFNγ was detected only in supernatant samples collected after culturing PBMCs with PHA, PBMCs of a healthy donor with non-modified allogeneic iTreg cells, as well as after co-cultivation of PBMCs of a healthy donor with B2M-knockouted allogeneic iTregs, but none of the TrAVs samples (Fig. 6D, 7D).

The concentration of IL-10 decreased in the following order: healthy donor PBMCs - healthy donor PBMCs plus autologous iTregs, healthy donor PBMCs plus TrAVs (Fig.
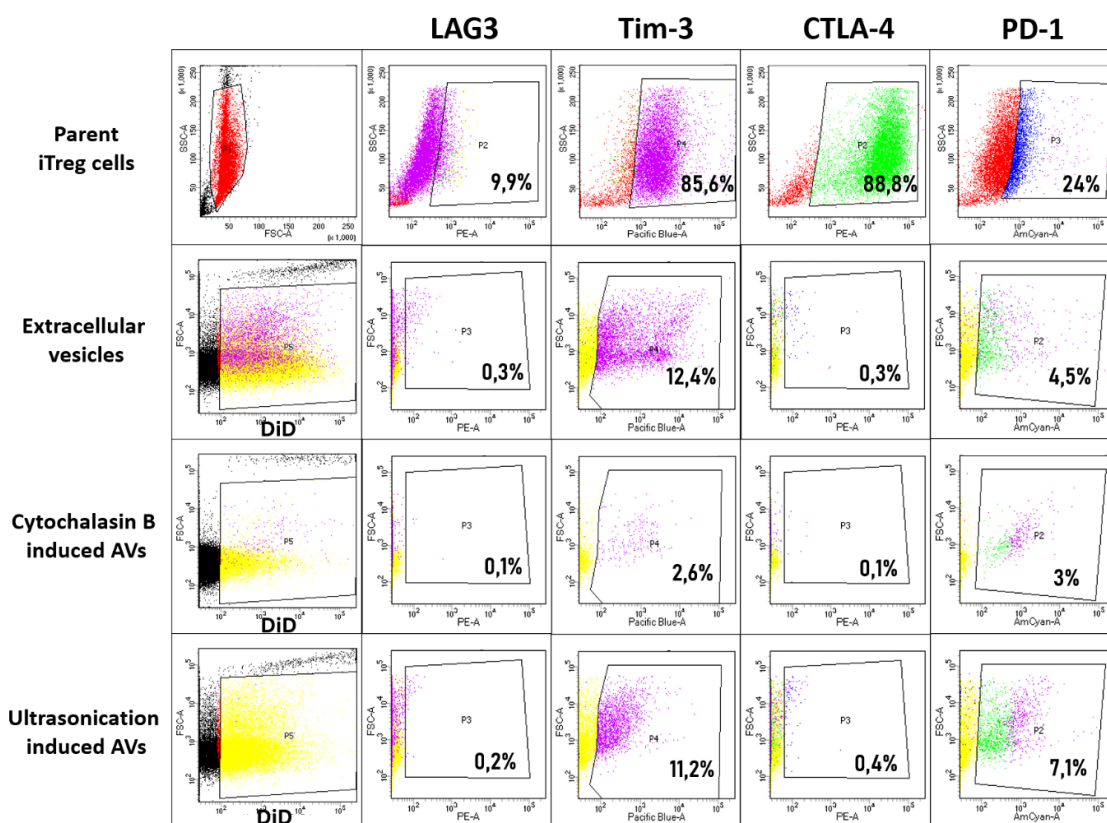
Fig. 4. Flow cytometry analysis of suppressor protein transfer from iTregs to vesicles. The expression of key immunosuppressive proteins—CTLA-4, PD-1, LAG-3, and Tim-3—was evaluated on three types of vesicles derived from iTregs: EVs, US TrAVs, and ChB TrAVs. Top row: Protein expression on iTregs used as parent cells. Second row: EVs. Third row: ChB TrAVs. Bottom row: US TrAVs. DiD membrane staining was applied for vesicle gating. The percentage of positively stained vesicles for each suppressor protein is displayed in the respective gate. The data illustrate the differential transfer of suppressor proteins, with US TrAVs showing higher levels of Tim-3 and PD-1 compared to ChB TrAVs and EVs.

6B). Also, during co-cultivation of healthy donor allogeneic PBMCs with non-modified TrAVs or allo TrAVs, the concentration of IL-10 was almost twice lower than during co-cultivation with its parent cell source (Fig. 7B).

Effect of healthy donor's artificial iTreg vesicles on activation of multiple sclerosis patient's PBMCs

On the last stage we estimated influence of healthy donor's non-modified iTregs and allo iTregs as well as obtained from allo TrAVs on PHA-induced activation of PBMCs, obtained from multiple sclerosis patients (Fig. 8).

No significant effect on the proportion of CD69 + PBMCs derived from MS patients was observed after co-cultivation with iTregs, allo iTregs and allo TrAVs (Fig. 8A). It also should be noted that the amount of CD69 + activated PBMSs was about twice lower in comparison with healthy donor from the previous section.

However, after co-cultivation of patients' PBMCs with iTregs, the concentration of IL-10 significantly increased, while a comparable slight increase was also observed after co-cultivation MS patients' PBMCs with allo iTregs and allo TrAVs (Fig. 8B).

A significant increase in IFNγ concentration was observed after co-cultivation of patient cells with iTregs and allo iTregs (Fig. 8D), while artificial vesicles did not

have such an effect, and the increase in IFNγ concentration in the medium was insignificant.

The concentration of IL-6 increased with co-cultivation of patients' PBMCs with iTregs, allo iTregs and allo TrAVs, while the degree of effect was different for each patient, and the maximum increase in IL-6 concentration was observed with co-cultivation of patient PBMCs with allo TrAVs (Fig. 8C).

Discussion

As we previously reported, ultrasonication and cytochalasin B both allow to generate artificial vesicles from T-cells carrying main functional proteins.[17] In this research we focused on artificial vesicles in the context of Tregs therapy of autoimmune diseases, in particular multiple sclerosis.

Multiple sclerosis is strongly associated with Treg cells dysfunction,[18] therefore the most promising approach seems to be allogeneic type of Tregs therapy with cells obtained from healthy donors. One more general obstacle for adoptive cell therapy by Tregs is the relative low amount of such a cell type in peripheral blood (about 5-7% of CD4 + T cells). Regarding these facts, we proposed a strategy of using in-vitro induced and expanded allo iTregs and allo US TrAVs as potential therapeutic agent
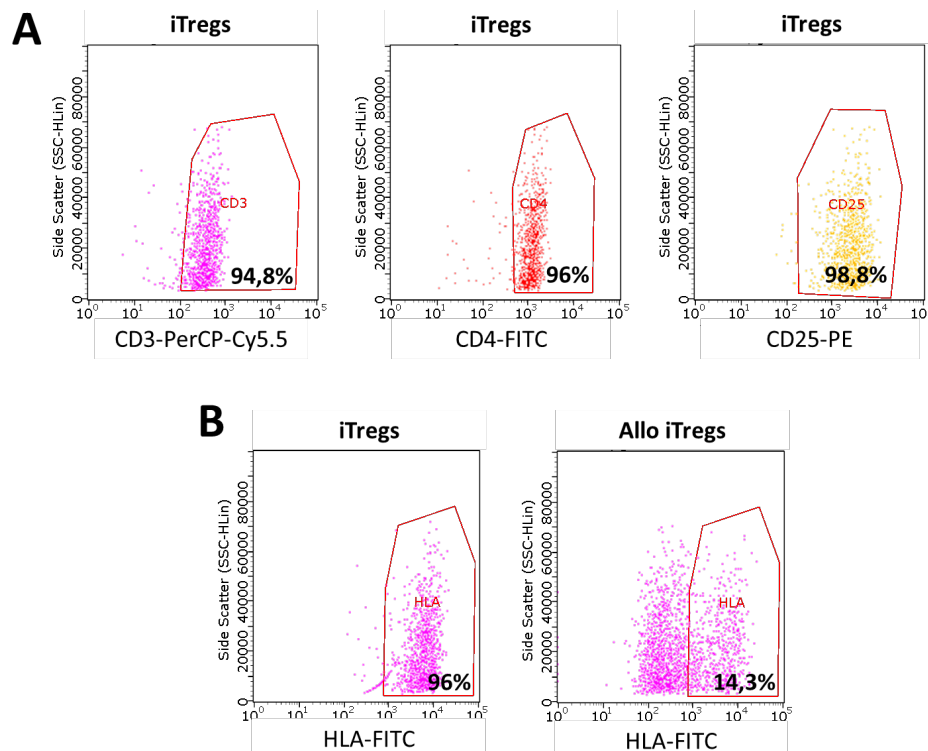
Fig. 5. Flow cytometry analysis of iTregs and B2M-knockdowned allo iTregs. (A) Validation of successful iTreg differentiation. Cells were stained with CD3, CD4, and CD25 to confirm the Treg phenotype. Gating shows a high proportion of $CD3^+CD4^+CD25^+$ cells, indicative of effective in vitro differentiation. (B) Assessment of *B2M* knockdown efficacy in allo iTregs. HLA-FITC staining was used to evaluate the expression of HLA class I molecules. Allo iTregs exhibited significantly reduced HLA expression compared to unmodified iTregs, confirming the successful knockdown of *B2M*.
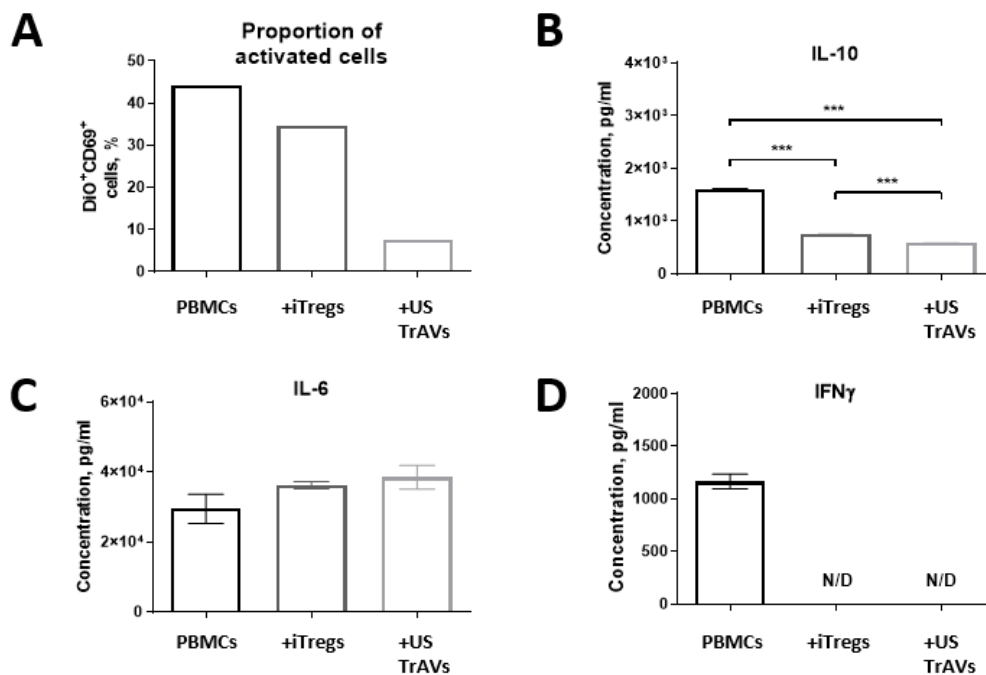

Fig. 6. Impact of iTregs and ultrasonication-induced artificial vesicles (US TrAVs) on the activation of autologous PBMCs from a healthy donor. (A) Flow cytometry analysis of CD69 + activated PBMCs. Co-cultivation with iTregs and US TrAVs significantly reduced the percentage of activated PBMCs compared to PHA-activated controls. (B) IL-10 concentrations in supernatants, as measured by ELISA. US TrAVs showed a significant reduction in IL-10 levels compared to iTregs. (C) IL-6 concentrations in supernatants. No significant changes were observed between groups. (D) IFNγ concentrations in supernatants. IFNγ was detected in the PHA-activated control but not in the co-cultivation groups (N/D, not detected). PBMCs were activated with 5 µg/mL PHA. DiO staining was used to distinguish PBMCs from iTregs during flow cytometry. Error bars represent standard deviations. Statistical significance is denoted as ***$P < 0.001$.
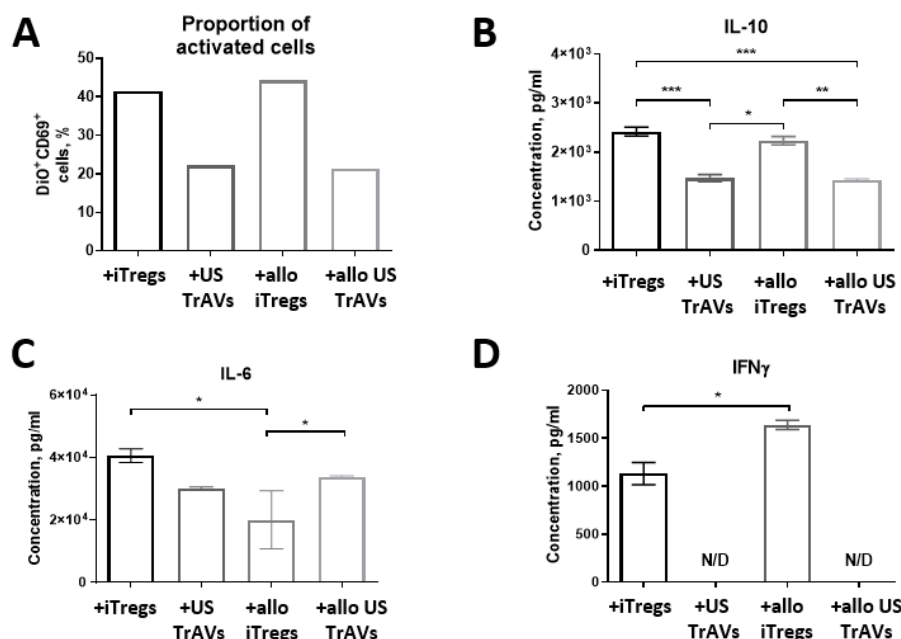
Fig. 7. Impact of iTregs, B2M-knockdowned iTregs (allo iTregs), and ultrasonication-induced artificial vesicles (US TrAVs and allo US TrAVs) on the activation of allogeneic PBMCs from a healthy donor. (A) Flow cytometry analysis of CD69 + activated PBMCs. Co-cultivation with iTregs, allo iTregs, US TrAVs, and allo US TrAVs resulted in varying levels of PBMC activation, with US TrAVs and allo US TrAVs showing the most significant suppression of CD69 + expression. (B) IL-10 concentrations in supernatants, as measured by ELISA. US TrAVs significantly reduced IL-10 secretion compared to iTregs, while allo iTregs and allo US TrAVs exhibited intermediate effects. (C) IL-6 concentrations in supernatants. IL-6 levels were modulated differently by the treatments, with a significant reduction observed in certain groups. (D) IFNγ concentrations in supernatants. IFNγ was detected in co-cultures with allo iTregs, whereas no detectable levels (N/D) were observed with US TrAVs or allo US TrAVs. PBMCs were activated with 5 µg/mL PHA. DiO staining was used to distinguish PBMCs from iTregs during flow cytometry. Error bars represent standard deviations, and statistical significance is denoted as *$P < 0.05$, ** $P < 0.01$, *** $P < 0.001$.

for patients with MS.

At the first stage we characterised and compared ChB TrAVs and US TrAVs. Scanning electron microscopy and nanoparticle tracking assay confirmed performance of both induction methods in point of iTregs, while NTA displays ultrasonication superiority over cytochalasin B and natural secretion in terms of induction of higher number of particles. As western-blot analysis demonstrates, obtained ChB TrAVs and US TrAVs don't belong to apoptotic bodies due to absence of marker caspase 3, contain small amount of cytosolic marker HSP70 and only US TrAVs carry endoplasmic reticulum. The presence of calnexin in US TrAVs can be explained by their production methodology: ultrasound stimulation causes micro-ruptures in cell membranes, leading to vesicle formation that incorporates surrounding cellular components. This mechanism accounts for the presence of the endoplasmic reticulum marker (calnexin) in vesicles generated through ultrasonic stimulation. Moreover, US TrAVs are more effective in transfer of one of the main T cell receptor CD3 than cytochalasin B induced TrAVs. All these characteristic data are consistent with previously obtained data for general T cells.[17]

Functional activity of TrAVs presumably strongly correlates with presence of functional important proteins characteristic for Tregs. For example, well-known PD-1 restrict self-antigen reaction[19] and CTLA-4 inhibits activity of T cells through competition with CD28,[20]

while newly investigated Tim-3 and LAG3 also play an important role in maintaining immune tolerance.[21] Flow cytometry performed for estimation of such functional proteins on TrAVs surface demonstrates that TrAVs induced by ultrasonication are enriched with Tim-3 and PD-1 in comparison with ChB-TrAVs. There is diverse evidence that the break of PD-1/PD1L axis participates in pathogenesis of multiple sclerosis[22] the same as Tim-3-ligand axis.[23] This observation was an additional point to give preference to ultrasonication for further functional investigation of TrAVs as a more effective method of artificial vesicles induction.

The next stage of research was to obtain allo TrAVs and evaluate its functional activity. The method of knockdown of B2M subunit of HLA I with shRNA reported to be an effective way for development of allogeneic cellular therapies which in combination with lentiviral delivery allow to achieve stable gene silencing[24] and seems to be quite suitable for our aims which were confirmed by us as high knockdown efficacy was reached.

CD69 is a marker of T cells activation involved in a pathway of a range of autoimmune diseases.[25] When co-cultured with PBMCs of healthy donor, autologous iTregs demonstrates slight decrease in number of CD69 + positive cells, while autologous TrAVs are much more effective from this point of view. This proportion is preserved during the transition to allo iTregs and TrAVs, but becomes less expressed and is not influenced by *B2M*
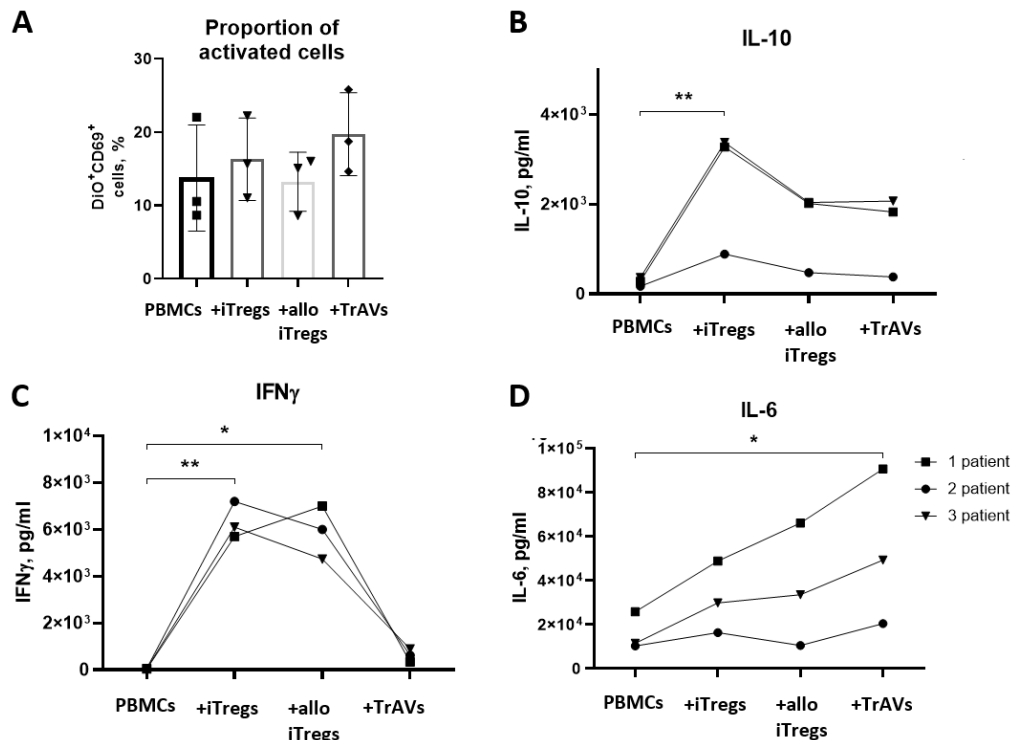
Fig. 8. Impact of iTregs, B2M-knockdowned iTregs (allo iTregs), and allo iTregs-derived ultrasonication-induced artificial vesicles (allo US TrAVs) from a healthy donor on the activation of PBMCs from multiple sclerosis patients. (A) Percentage of activated CD69⁺PBMCs, as determined by flow cytometry. Activation levels varied across treatments, with allo US TrAVs showing moderate suppression compared to allo iTregs. (B) IL-10 concentrations in supernatants measured by ELISA. Significant differences in IL-10 levels were observed, with allo iTregs and allo US TrAVs promoting an increase compared to controls. (C) IL-6 concentrations in supernatants measured by ELISA. IL-6 levels were elevated in all co-cultivation groups, with the highest increase observed in allo US TrAVs-treated cells. (D) IFNγ concentrations in supernatants measured by ELISA. IFNγ production was significantly lower in allo US TrAV-treated PBMCs compared to iTregs and allo iTregs. PBMCs were activated with 5 µg/mL PHA. DiO staining was applied to distinguish patient-derived PBMCs from donor-derived cells during flow cytometry. Statistical significance is denoted as * $P < 0.05$ and **$P < 0.01$. Error bars represent standard deviations.

knockdown.

At the same time, cytokines secretion also demonstrates correlated effects of iTregs and TrAVs on autologous PBMCs of healthy donor activation through IFNγ and IL-10 downregulation which could be an evidence of usage of some common mechanism of immunomodulation for TrAVs and its parent cells. Moving to allogeneic co-cultivation such a downregulation also remained for TrAVs, but not iTreg cells, which probably means that TrAVs has lower immunogenicity than parent cells without correlation with B2M status.

Moving towards evaluation of healthy donor's TrAVs influence on activation of PBMCs of patients with MS, only TrAVs, but not iTregs, demonstrate strong downregulation of IFNγ secretion. Despite the fact that the role of IFNγ in MS progression is still under discussion, classically IFNγ production is considered as a driver of inflammation and autoimmunity, including MS.[26] This observation also supports the potential of TrAVs as immunoregulation agents. Balance of IL-6 and IL-10 is a more complex question in the context of autoimmunity. TrAVs demonstrate the same impact on IL-10 levels as parent iTregs, but relative upregulation of IL-6. Mechanism of such influence seems to be unclear, especially taking

into account the fact that MS patients have deficient IL-6/IL-10 axis. From a practical point of view regarding IL-10 TrAVs efficiency is comparable with iTregs which can be estimated as a good mark for its therapeutic potential, while IL-6 raise is rather a disadvantage.[27] It is interesting to note that the shape of IL-6 dynamics between samples correlates with CD69 + expression for patients' PBMC but is absolutely controversial for healthy donor, which can be caused by immunosuppressive therapy pressure and highlights the differences in immune cells functioning between these groups. This effect appears biologically significant, warranting further investigation. Future studies elucidating the mechanisms underlying IL-6 elevation will facilitate better understanding of associated therapeutic risks and potential mitigation strategies.

Conclusion

The development of effective therapies for autoimmune diseases, including MS, remains a significant challenge in modern immunology. While cellular therapies have demonstrated success in oncology and regenerative medicine, their application in MS is hindered by several obstacles, including the dysfunction of Tregs and the difficulty of ensuring their delivery to the CNS. A

promising alternative is the use of allogeneic EVs, which offer a cell-free therapeutic modality with potential advantages such as scalability, reduced immunogenicity, and the ability to cross the blood-brain barrier.

In this study, we developed a novel approach for the efficient production of allogenic TrAVs derived from in iTregs and performed a preliminary assessment of their functional properties. Our results demonstrate that TrAVs not only retain key immunosuppressive features of their parent cells but also exhibit a significant capacity to modulate immune responses, particularly in the context of PBMCs activation. These findings highlight the potential of TrAVs as a scalable and biosafe therapeutic alternative for MS and other autoimmune diseases.

However, while these initial results are encouraging, further research is needed to elucidate the mechanisms underlying TrAV-mediated immunomodulation, optimize their production process, and evaluate their therapeutic efficacy in preclinical and clinical models. The promising outcomes of this study pave the way for future investigations into the broader application of artificial vesicles in the treatment of autoimmune diseases.

Authors' Contribution
Conceptualization: Irina Alekseevna Ganeeva, Ekaterina Anatolievna Zmievskaya, Emil Rafaelevich Bulatov.
Data curation: Irina Alekseevna Ganeeva, Elvina Maratovna Gilyazova, Arthur Ajdarovich Khannanov, Mariia Eugenievna Nektorova, Alexey Michailovich Rogov.
Formal analysis: Irina Alekseevna Ganeeva, Arthur Ajdarovich Khannanov, Ekaterina Anatolievna Zmievskaya.
Funding acquisition: Ekaterina Anatolievna Zmievskaya.
Investigation: Ekaterina Anatolievna Zmievskaya.
Methodology: Irina Alekseevna Ganeeva, Arthur Ajdarovich Khannanov, Alexey Michailovich Rogov, Timur Ildarovich Khaibullin, Ekaterina Anatolievna Zmievskaya, Emil Rafaelevich Bulatov.
Project administration: Ekaterina Anatolievna Zmievskaya, Emil Rafaelevich Bulatov.
Resources: Emil Rafaelevich Bulatov.
Supervision: Emil Rafaelevich Bulatov.
Validation: Ekaterina Anatolievna Zmievskaya.
Visualization: Ekaterina Anatolievna Zmievskaya.
Writing–original draft: Irina Alekseevna Ganeeva, Ekaterina Anatolievna Zmievskaya.
Writing–review & editing: Mariia Eugenievna Nektorova, Ekaterina Anatolievna Zmievskaya, Emil Rafaelevich Bulatov.

References
1. Manu MS, Hohjoh H, Yamamura T. Extracellular vesicles as pro- and anti-inflammatory mediators, biomarkers and potential therapeutic agents in multiple sclerosis. *Aging Dis* **2021**; 12: 1451-61. doi: 10.14336/ad.2021.0513.
2. Chasov V, Zmievskaya E, Ganeeva I, Gilyazova E, Davletshin D, Khaliulin M, et al. Immunotherapy strategy for systemic autoimmune diseases: betting on CAR-T cells and antibodies. *Antibodies (Basel)* **2024**; 13: 10. doi: 10.3390/antib13010010.
3. Baecher-Allan C, Kaskow BJ, Weiner HL. Multiple sclerosis: mechanisms and immunotherapy. *Neuron* **2018**; 97: 742-68. doi: 10.1016/j.neuron.2018.01.021.
4. Bar-Or A, Li R. Cellular immunology of relapsing multiple sclerosis: interactions, checks, and balances. *Lancet Neurol* **2021**; 20: 470-83. doi: 10.1016/s1474-4422(21)00063-6.
5. Azimi M, Ghabaee M, Naser Moghadasi A, Noorbakhsh F, Izad M. Immunomodulatory function of Treg-derived exosomes is impaired in patients with relapsing-remitting multiple sclerosis. *Immunol Res* **2018**; 66: 513-20. doi: 10.1007/s12026-018-9008-5.
6. Chwojnicki K, Iwaszkiewicz-Grześ D, Jankowska A, Zieliński M, Łowiec P, Gliwiński M, et al. Administration of CD4(+) CD25(high)CD127(-)FoxP3(+) regulatory T cells for relapsing-remitting multiple sclerosis: a phase 1 study. *BioDrugs* **2021**; 35: 47-60. doi: 10.1007/s40259-020-00462-7.
7. Xu J, Zhang J, Zhang Z, Gao Z, Qi Y, Qiu W, et al. Hypoxic glioma-derived exosomes promote M2-like macrophage polarization by enhancing autophagy induction. *Cell Death Dis* **2021**; 12: 373. doi: 10.1038/s41419-021-03664-1.
8. Li Y, Zhu X, Zhang M, Tong H, Su L. Heatstroke-induced hepatocyte exosomes promote liver injury by activating the NOD-like receptor signaling pathway in mice. *PeerJ* **2019**; 7: e8216. doi: 10.7717/peerj.8216.
9. Busatto S, Morad G, Guo P, Moses MA. The role of extracellular vesicles in the physiological and pathological regulation of the blood-brain barrier. *FASEB Bioadv* **2021**; 3: 665-75. doi: 10.1096/fba.2021-00045.
10. Ramos-Zaldívar HM, Polakovicova I, Salas-Huenuleo E, Corvalán AH, Kogan MJ, Yefi CP, et al. Extracellular vesicles through the blood-brain barrier: a review. *Fluids Barriers CNS* **2022**; 19: 60.

Research Highlights

What is the current knowledge?
- Multiple sclerosis is an autoimmune disease related with regulatory T cells dysfunction.
- Adoptive cellular therapy of autoimmune diseases is a promising approach.
- Extracellular vesicles as a therapeutic modality have a number of advantages over cellular therapy but meet technological obstacles.

What is new here?
- Ultrasonication is an effective method of artificial vesicles induction from T regulatory cells.
- Artificial vesicles induced from T regulatory cells by ultrasonication carry functional important immunosuppressive proteins.
- Artificial vesicles induced from T regulatory cells by ultrasonication reduce in vitro activation of PBMCs obtained from healthy donor or patients with multiple sclerosis.

doi: 10.1186/s12987-022-00359-3.

11. Banks WA, Sharma P, Bullock KM, Hansen KM, Ludwig N, Whiteside TL. Transport of extracellular vesicles across the blood-brain barrier: brain pharmacokinetics and effects of inflammation. *Int J Mol Sci* **2020**; 21: 4407. doi: 10.3390/ijms21124407.

12. Gutiérrez-Fernández M, de la Cuesta F, Tallón A, Cuesta I, Fernández-Fournier M, Laso-García F, et al. Potential roles of extracellular vesicles as biomarkers and a novel treatment approach in multiple sclerosis. *Int J Mol Sci* **2021**; 22: 9011. doi: 10.3390/ijms22169011.

13. Syromiatnikova V, Prokopeva A, Gomzikova M. Methods of the large-scale production of extracellular vesicles. *Int J Mol Sci* **2022**; 23: 10522. doi: 10.3390/ijms231810522.

14. Mendez R, Banerjee S. Sonication-based basic protocol for liposome synthesis. *Methods Mol Biol* **2017**; 1609: 255-60. doi: 10.1007/978-1-4939-6996-8_21.

15. Zhao Z, Qu L, Shuang T, Wu S, Su Y, Lu F, et al. Low-intensity ultrasound radiation increases exosome yield for efficient drug delivery. *J Drug Deliv Sci Technol* **2020**; 57: 101713. doi: 10.1016/j.jddst.2020.101713.

16. Ambattu LA, Ramesan S, Dekiwadia C, Hanssen E, Li H, Yeo LY. High frequency acoustic cell stimulation promotes exosome generation regulated by a calcium-dependent mechanism. *Commun Biol* **2020**; 3: 553. doi: 10.1038/s42003-020-01277-6.

17. Zmievskaya EA, Mukhametshin SA, Ganeeva IA, Gilyazova EM, Siraeva ET, Kutyreva MP, et al. Artificial extracellular vesicles generated from t cells using different induction techniques. *Biomedicines* **2024**; 12: 919. doi: 10.3390/biomedicines12040919.

18. Raffin C, Vo LT, Bluestone JA. Treg cell-based therapies: challenges and perspectives. *Nat Rev Immunol* **2020**; 20: 158-72. doi: 10.1038/s41577-019-0232-6.

19. Gianchecchi E, Fierabracci A. Inhibitory receptors and pathways of lymphocytes: the role of PD-1 in Treg development and their involvement in autoimmunity onset and cancer progression. *Front Immunol* **2018**; 9: 2374. doi: 10.3389/fimmu.2018.02374.

20. Mitsuiki N, Schwab C, Grimbacher B. What did we learn from CTLA-4 insufficiency on the human immune system? *Immunol Rev* **2019**; 287: 33-49. doi: 10.1111/imr.12721.

21. Lu C, Tan Y. Promising immunotherapy targets: TIM3, LAG3, and TIGIT joined the party. *Mol Ther Oncol* **2024**; 32: 200773. doi: 10.1016/j.omton.2024.200773.

22. Li H, Zheng C, Han J, Zhu J, Liu S, Jin T. PD-1/PD-L1 axis as a potential therapeutic target for multiple sclerosis: AT cell perspective. *Front Cell Neurosci* **2021**; 15: 716747. doi: 10.3389/fncel.2021.716747.

23. Chen H, Zha J, Tang R, Chen G. T-cell immunoglobulin and mucin-domain containing-3 (TIM-3): solving a key puzzle in autoimmune diseases. *Int Immunopharmacol* **2023**; 121: 110418. doi: 10.1016/j.intimp.2023.110418.

24. Zhang X, Jin X, Sun R, Zhang M, Lu W, Zhao M. Gene knockout in cellular immunotherapy: application and limitations. *Cancer Lett* **2022**; 540: 215736. doi: 10.1016/j.canlet.2022.215736.

25. Mahdavi Gorabi A, Hajighasemi S, Kiaie N, Gheibi Hayat SM, Jamialahmadi T, Johnston TP, et al. The pivotal role of CD69 in autoimmunity. *J Autoimmun* **2020**; 111: 102453. doi: 10.1016/j.jaut.2020.102453.

26. Arellano G, Ottum PA, Reyes LI, Burgos PI, Naves R. Stage-specific role of interferon-gamma in experimental autoimmune encephalomyelitis and multiple sclerosis. *Front Immunol* **2015**; 6: 492. doi: 10.3389/fimmu.2015.00492.

27. Ireland SJ, Monson NL, Davis LS. Seeking balance: Potentiation and inhibition of multiple sclerosis autoimmune responses by IL-6 and IL-10. *Cytokine* **2015**; 73: 236-44. doi: 10.1016/j.cyto.2015.01.009.